Solar Energy Materials & Solar Cells 262 (2023) 112526

Contents lists available at ScienceDirect

Solar Energy Materials and Solar Cells

journal homepage: www.elsevier.com/locate/solmat

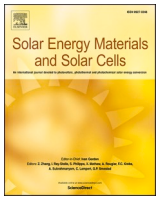

The effect of storage conditions on the long-term stability of ethylene-vinyl-acetate (EVA) copolymer used in glass/glass modules

Luca Gnocchi [a,*], Alessandro Virtuani [a], Andrew Fairbrother [a], Eleonora Annigoni [b], Christophe Ballif [a,c]

[a] École Polytechnique Fédérale de Lausanne (EPFL), Institute of Electrical and Microengineering (IEM), Photovoltaics and Thin Film Electronics Laboratory (PV-Lab), 2000, Neuchâtel, Switzerland
[b] Holland Innovative, High Tech Campus 29, 5656 AE, Eindhoven, the Netherlands
[c] Swiss Center for Electronics and Microtechnology (CSEM), SE-center, CH-2002, Neuchâtel, Switzerland

A B S T R A C T

We evaluate the effect of storage conditions of uncured encapsulant rolls and the potential consequences on photovoltaic (PV) module performance. We show the impact of residual water trapped inside laminated double glass PV modules after lamination and during UV exposure. We focus on ethylene vinyl acetate (EVA) copolymer and its stability over 630 kWh/m^2 UV exposure (equivalent to 10 years of outdoor exposure in a Central European country). Three storage conditions were tested by simulating different moisture contents to mimic relative humidity variations that can occur when polymeric foils are exposed to an uncontrolled environment, such as the PV module production line, next to the laminator machine. The presence of water during lamination had no apparent impact on module quality and performance after the fabrication but only became apparent during the aging test. The module power loss was directly related to the EVA chemical and physical degradation and varied depending on the storage history. Results indicate that when the storage is not too harsh, its effect can be somehow mitigated. Based on our observations, we leave a door open to the adoption of high-quality EVA polymers in the manufacturing of glass-glass modules. However, the storage and handling conditions prescribed by the supplier should be carefully respected.

1. Introduction

The choice of a proper encapsulant is critical to ensuring optimal long-term performance of a module [1]. This is even more important with the rise of the solar cells with passivation layers, including passivated Emitter and Rear Cells (PERC) and silicon heterojunction (SHJ) cells, for which, bifacial devices can be processed and encapsulated in a glass-glass (G-G) laminate. The G-G layout have been previously used mostly for thin-film PV technologies [2] and BI-PV products. Nevertheless, this structure is gaining momentum in the last few years [3].

Despite not being the best performing encapsulant, Ethylene Vinyl Acetate copolymer (EVA) is still the primary polymer in use in the PV industry thanks to its long track record and good quality-price ratio. The instability issues of EVA during long-term outdoor exposure are, however, well documented in literature [4–7]. UV radiation, moisture, and exposure to elevated temperatures are all stress factors that may lead to a degradation of polymers. This may induce a discoloration of the material, with reduction of transparency and consequently of the photocurrent of the module. Acetic acid is one of the by-products of EVA degradation. In the presence of moisture and heat, a hydrolysis reaction will occur to produce acetic acid [8], lowering the pH and potentially leading to a corrosion of the metallic interconnections [9]. Moreover, with the addition of the UV radiation, the photodegradation initiates faster from vulnerable vinyl acetate groups, followed by further degradation in the main chain by Norrish type chemical reactions [10]. The EVA formulation has improved over the years with the modification of additives to reduce the degradation rate.

Material and process quality are critical to product quality and lifetime at all manufacturing stages, including before production. In fact, a PI Berlin survey of over 250 PV manufacturers observed that material storage and preparation is a major factor for a good PV module manufacturing quality [11]. Additionally, the limited number of modules (typically less than 10) tested by the manufacturer for qualification certificate is not representative of the whole production amount [12] and assumed flawless modules could instead rapidly degrade after installation because of poor material quality. It is good practice to store uncured rolls of encapsulants in dark, dry (relative humidity, RH <50%), and cool place (<30 °C) before they are used [13]. Moreover, some encapsulant manufacturers state that the rolls should not be stored

* Corresponding author.
E-mail address: lucagnocchi90@icloud.com (L. Gnocchi).

https://doi.org/10.1016/j.solmat.2023.112526
Received 27 April 2023; Received in revised form 20 August 2023; Accepted 23 August 2023
Available online 2 September 2023

for more than six months and that active humidity control is necessary after the roll is open [14]. However, proper storage conditions are not always maintained, and seasonal variations in temperature and humidity may be present in the storage room or the manufacturing line. Additionally, after the roll is removed from its packaging, it should be used in a short time interval. Prolonged exposure to an uncontrolled environment and its usage after the recommended expiration date can affect the long-term performance of the module. Loss of adhesion, non-uniform cross-linking, and ultimately faster module power loss are reported as consequences of a low-quality encapsulant [15–17].

2. Method and approach

We manufactured single-cell glass-glass modules using conventional Al-BSF (Aluminum Back Surface Field) crystalline silicon (c-Si) cells and a commercial, low UV cut-off EVA formulation. This formulation is the more befitting a double glass structure [18]. The choice of Al-BSF cells was motivated by their presumed better UV stability compared to newer architectures, such as PERC and SHJ [19,20]. This allowed us to exclude the possibility of UV-induced cell degradation and instead attribute module changes to encapsulant degradation. Before lamination, the uncured encapsulant polymer sheets, were and stored in different conditions to simulate daily/seasonal variations that might occur if they are not kept under controlled temperature and humidity conditions. After lamination, modules were subjected to accelerated UV aging tests, where they were exposed to a cumulative UV dose of up to 630 kWh/m^2, corresponding to an outdoor exposure of about 10 years in a mid-latitude country with a temperate climate, such as Switzerland (~60 kWh/m^2/y of UV). The electrical performance and material changes were monitored periodically.

2.1. Storage conditions

Polymer manufacturers give optimal storage conditions for PV encapsulants [14]. For EVA, in general, an optimum temperature of 22 °C and a relative humidity ≤50% are recommended after the roll is open [13]. In our experiment, the encapsulant foils were cut in 20 × 20 and 7 × 7 cm^2 squared samples and subjected to three different preconditioning conditions before lamination (see Table 1) to simulate seasonal humidity variations that may occur in a manufacturing line or under non-optimal storage conditions. The EVA-30 foil corresponds to an uncured encapsulant roll stored under optimal conditions, as recommended by the supplier: the storage room was kept at constant relative humidity and temperature in the dark. EVA-65 reflects the situation in which the roll was kept in an uncontrolled indoor environment with a high RH. This was done by storing polymeric sheets inside a climatic chamber. The EVA-100 encapsulant is an extreme condition in which the roll was soaked in water. This last condition was decided upon previous tests where the desorption of water during the sample preparation was measured (see Supporting information, Section 1). Desorption of water for EVA-65 inevitably occurs in the time between removal from the climate chamber, module layup, and lamination process. Therefore, while the EVA-100 storage conditions are certainly unlikely, they ensure that moisture is present during the lamination process.

2.2. Samples design and fabrication

For each of the three EVA storage conditions, single-cell modules (20 × 20 cm^2) with c-Si Al–BFS cells were manufactured (glass/EVA/cell/EVA/glass) to monitor the impact of storage conditions on module performance. A 3.2 mm thick heat strengthened SOLARFLOAT HT glass was used. Additionally, 7 × 7 cm^2 coupons were prepared in order to check the degradation of the EVA. Some characterization techniques require extraction of the EVA, therefore two different sample structures were used (Fig. 1):

1. Glass/EVA/EVA/glass: EVA laminates to monitor encapsulant degradation, specifically the optical transmittance (Fig. 1a).
2. Glass/EVA/ETFE/Glass: EVA laminates with an ETFE "release layer". This allowed "opening" of the modules for FTIR and DSC (Fig. 1b).

Table 1
EVA storage conditions.

ID code	Storage Temperature [°C]	Rel. Humidity [%]	Storage time [days]
EVA-30	20	30	5
EVA-65	30	65	5
EVA_100	20	Soaked in water	5

2.3. Aging conditions

All laminates were aged using the IEC 62788-7-2 standard with A3 conditions for a total duration of 10000 h. The setting inside the climatic chambers along with the test duration are reported in Table 2. The Xe-arc lamp with daylight filter has a UV dose corresponding to 63 W/m^2 (295–395 nm range).

2.4. Module inspection and performance

Visual images of samples were taken to check their appearance. The module performance was investigated by means of illuminated current-voltage (I–V) characteristics performed at standard test conditions (STC: AM1.5G, 25 °C, 1000 W/m^2) using a LED-halogen based sun simulator. Electroluminescence images were taken with the modules biased under maximum power point.

2.5. EVA properties

UV–visible (UV–vis) spectroscopy was used to characterize the optical properties of the polymer by analysing G/EVA/G coupons (laminate in Fig. 1a). Spectra were recorded from 250 to 800 nm.

To assess the effect of UV exposure on the structure of EVA, Fourier Transformed Infrared (FTIR) in attenuated total reflection (ATR) mode was used (laminate in Fig. 1b). The spectra were recorded over the range 650–4000 cm^{-1}. The measurements were obtained from an average of 64 scans.

Finally, differential scanning calorimetry (DSC) measurements were made on to verify changes in the crystal morphology and stability of the EVA (laminate in Fig. 1b). Thermograms were recorded from −30 °C to 225 °C, under a nitrogen atmosphere (80 ml/min), and the heating and cooling rate was 10 K/min. Samples of about 10 mg weight were cut from the laminate in Fig. 1b.

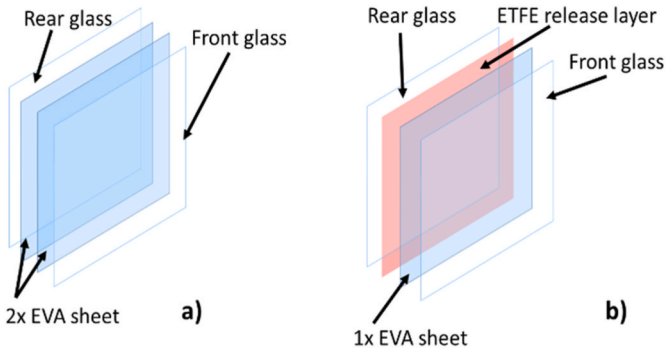

Fig. 1. Schematic of the coupons used to investigate the degradation of the EVA during UV aging: (a) G/EVA/G was used to study the optical properties; (b) G/EVA/ETFE/G was used for invasive techniques analysis such as FITR-ATR and DSC -due to the possibility of opening up the sample.

Table 2
Aging test parameters.

TestStandard	Air temperature [°C]	Black panel temperature [°C]	Relative humidity [%]	UV intensity (@ 340 nm) [W/m^2]	Duration [h – kWh/m^2]
IEC 62788-7-2, A3	65	90	20	0.8	10000 – 630

2.6. Water ingress simulation

We run some mathematical simulations to complete our work. We solved by 2D Finite Element Method (FEM) the Fick's second Law of Diffusion as reported in Refs. [21–23]. The diffusion coefficients of EVA used in the simulation were experimentally determined following the procedure explained in Ref. [21]. The diffusion of moisture inside a standard 60 cells module was evaluated in 2 different climates, during 20 years of outdoor exposure.

3. Results

3.1. EVA storage effect after lamination process – non aged samples

3.1.1. Module inspection and performance

After the lamination process, the module manufactured with the EVA-30 encapsulant did not show any visible defects. In contrast, the modules stored under non-optimal conditions revealed a few minor aesthetic defects. As reported in Fig. 2, modules encapsulated with EVA-65 and EVA-100 resulted in bubble formation along the edges, while visual quality above the cell appears normal. The higher the RH during the storage, the higher the dimensions and density of the bubbles, increasing in size from few millimeters up to 1 cm, for EVA-65 and EVA-100, respectively. The cell performance and properties (I–V and EL) showed no differences.

3.1.2. EVA properties after lamination

The optical transmittance of the glass/polymer/glass samples manufactured with the three encapsulants did not show any difference between 250 and 800 nm (results not reported here). This result is in good agreement with the fact that no difference was observed in the electrical performance of the modules manufactured with the same encapsulants.

The characterization of the chemical groups via FTIR spectroscopy for the three different stored EVA after lamination revealed characteristic bands for the unaged samples (Fig. 3).

Typical peaks for EVA at 1370, 1463, 2850, and 2920 cm^{-1} can be assigned to the symmetric, asymmetric and deformation vibrations of the CH_2 and CH_3 groups of the ethylene segments [24]. The absorption at 1736, 1238 and 1020 cm^{-1} correspond to ester groups of the Vinyl Acetate segments [24]. The effect of the storage condition was most noticeable by the increase of the peak at 1695 cm^{-1}, and became more

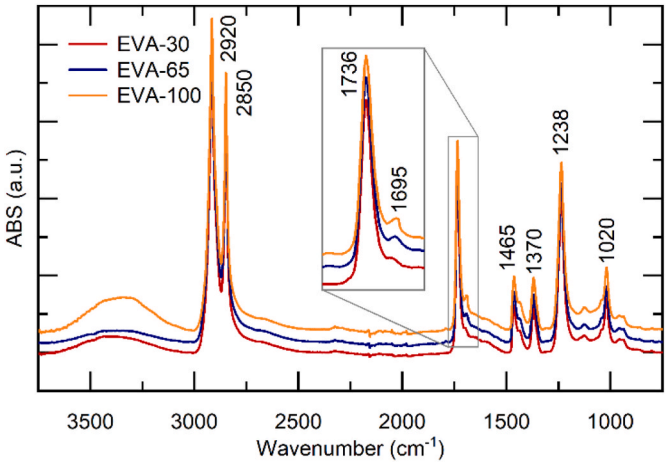

Fig. 3. FTIR-ATR scans performed on the EVA encapsulant stored at different conditions (EVA-30, EVA-65, and EVA-100) after the lamination process. The zoom in highlights the increase in intensity of the peak at 1695 cm−1 attributed to C═O of a carboxylic group.

pronounced going from EVA-65 to EVA-100. It can be attributed to C═O of a carboxylic group [25]. This means that the pre-absorbed moisture during simulated uncontrolled storage was already sufficient to trigger the generation of acetic acid. The presence of trapped water in EVA-100 was also well visible in the far IR range from 3000 to 3500 cm^{-1}, a broad peak assigned to –OH groups.

Fig. 4a compares the DSC curves of EVA-30, EVA-65 and EVA-100 recorded after the lamination. The first heating scan gives information relative to the history of the polymer, including both physical and chemical characteristics (i.e. lamination or aging effects). Following a cooling step, the second heating process is meant to erase the thermal history of the sample and reveals only irreversible processes (i.e. chemical degradation). During the first heating step, EVA-30 shows the typical broad melting region for EVA with melting peaks at 46 °C and 65 °C [26] with an inset temperature at 42 °C. These peaks are related to the existence of two predominant crystal sizes. The lower melting peak is usually named secondary crystallization peak. It is assigned to the melting of small ethylene crystals embedded in vinyl acetate (VA) units.

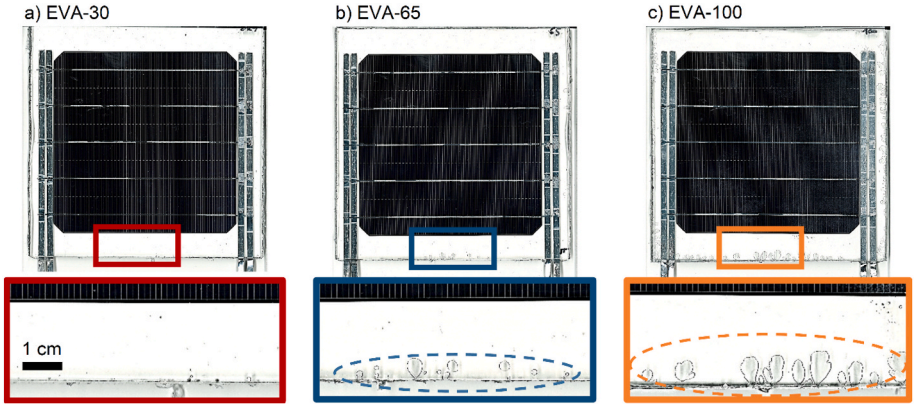

Fig. 2. Visual inspection of single-cell modules encapsulated with a) EVA-30, b) EVA-65, and c) EVA-100, performed after the lamination process, highlighting the presence of bubbles for laminates encapsulated with poorly stored EVAs.

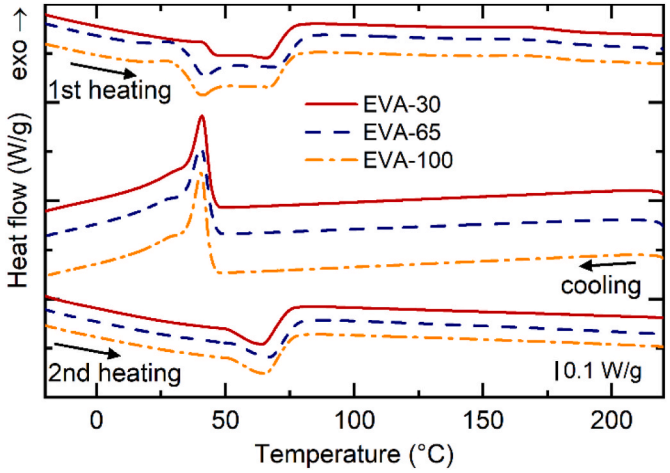

Fig. 4. DSC thermographs performed on the G/ETFE/EVA/G coupons with EVAs stored at different conditions after the lamination process.

The second corresponds to highly organized crystal polyethylene chains [26]. The other samples with EVA in non-optimal storage conditions (EVA-65, EVA-100) had a comparably less stable crystal phase that melts at lower temperature with respect to the EVA-30. The melting temperature of the secondary crystallization peak decreases down to 41 °C. Additionally, the primary over secondary crystallization intensity ratios (CIR) were calculated: EVA-30 had the highest CIR of 1.55, whereas EVA-65 and EVA-100 encapsulants exhibited a lower value of 0.79. However, this effect was erased after the first cycle. The cooling and second heating scans show the same trends for all three conditions: the crystallization peak is set at 40 °C during the cooling. The EVA starts to melt again at around 65 °C (primary crystallization melting peak) when heated up the second time. The differences in the lower temperature melting peak and the comparable higher peak related to the second crystallization melting of EVA-65 and EVA-100 (i.e. same CIR) reveal that, regardless the RH level, a prolonged uncontrolled storage of the uncured encapsulant affects the morphological properties of the EVA developed during the curing process. The reduction of the secondary crystallization melting peak is a typical result in samples aged in damp heat conditions (i.e. 85 °C and 85%RH) as reported by Ottersbock and Oreski [27,28]. When moisture is present, the ethylene segments in VA moieties are less perfect and tend to form smaller and less stable crystals.

3.2. EVA storage effect during UV aging

3.2.1. Aged modules inspection and performance

During UV exposure, the visual appearance and the electrical performance of the single-cell modules were checked at regular intervals.

Fig. 5 shows images from the visual inspections of the modules laminated with the three different EVA preconditioning after 15 kWh/m^2 (i.e. after 250 h of aging test). By comparing these images with the ones taken directly after the lamination (see Fig. 2), it is clear that the preconditioning had a direct effect on the aesthetic of the module, particularly on the encapsulant morphology. For the well-stored polymer (i.e. EVA-30 in Fig. 5a) no defects were observed. On the module using EVA-65 (Fig. 5b), it can be observed that the bubbles that had initially formed along the edges of the module were gettered and evacuated from the laminate. However, the extreme condition represented in the EVA-100 module (Fig. 5c) reveals a different morphology: new bubbles were formed and pre-existing bubbles expanded, creating a network of channels across the whole module. Fig. 6 shows the I–V curves of single-cell modules encapsulated with EVA-30 and the related transmittance measured on G/EVA/G coupons. For modules with EVA-30 and EVA-65 the electrical performance was stable during the whole aging experiment duration (i.e. up to 630 kWh/m^2).

However, for the EVA-100 module UV radiation had a major effect on performance. As represented in Fig. 7, the power output of this

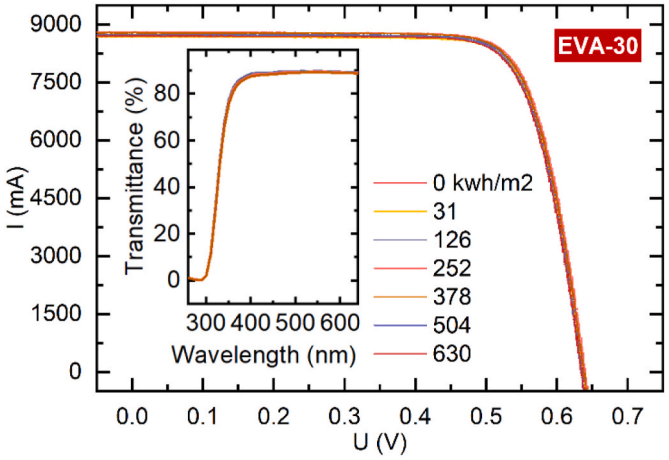

Fig. 6. I–V curves of single-cell module and transmittance measurements of G/EVA/G samples encapsulated with well stored EVA-30, during UV aging (up to a total UV dose of 630 kWh/m^2).

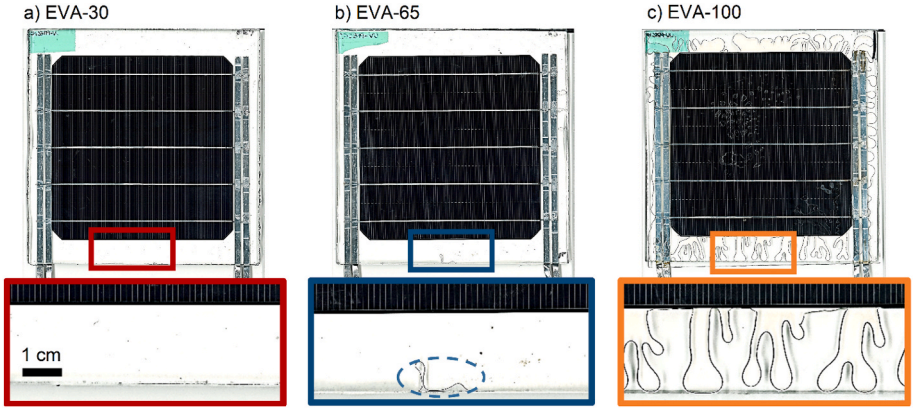

Fig. 5. Visual inspection of single-cell modules, performed during aging test (i.e. 15 kWh/m^2 UV dose). Sample encapsulated with EVA-30 (a), show no visual defects; in module encapsulated with EVA-65 (b) bubbles generated after lamination are gettered and evacuated from the edges; laminate with EVA-100 (c) clearly show that bubbles spread along the whole module perimeter.

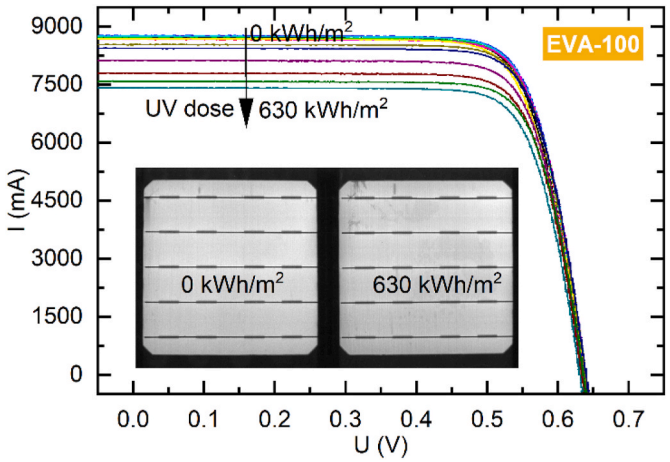

Fig. 7. I–V curves and EL images of single-cell module encapsulated with EVA-100 during UV aging (up to a total UV dose of 630 kWh/m^2).

sample remained stable up to a cumulative UV dose of about 200 kWh/m^2, followed by a constant reduction of the current when exposed at higher UV doses. All other cell parameters remained unchanged (e.g. fill factor, and open circuit voltage). No corrosion was detected on the ribbons, and EL images (Fig. 7) indicate the Al-BSF solar cell remained stable up to a UV dose of 630 kWh/m^2.

The optical measurements in Fig. 8a show the transmittance of the encapsulant EVA-100 constantly decreasing in the low wavelength range starting from a dose of 189 kWh/m^2. The yellowness index (Y.I.) can be calculated, which was found to correlate with the cell current loss (Fig. 8b). From this, it can be said that the current reduction on the module encapsulated with EVA-100 is an effect of the encapsulant discoloration, which blocks light from reaching the cell, and not corrosion or other effects.

3.2.2. *Variation of EVA properties during UV test*

The transmittance of EVA-30 and EVA-65 was unchanged during the UV test. This contrasted with the significant changes to optical properties of EVA-100, described above in correlation to the module performance (Fig. 8a and b).

The IR peaks of the EVA-30 and EVA-65 encapsulants from FTIR were similar during UV aging. The peaks remained stable during the whole aging test, up to a total UV dose of 630 kWh/m^2, without any sign

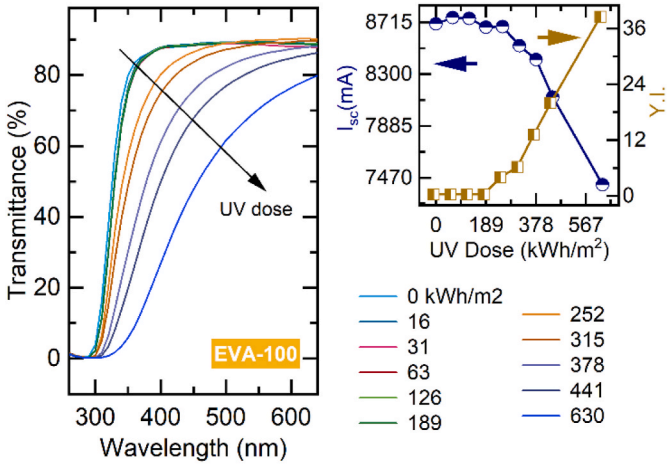

Fig. 8. a) Transmittance changes in the UV–Vis range of the G/EVA/G coupon with EVA-100 and b) correlation between Isc and Yellowness index of the one-cell module laminated with EVA-100 during UV aging, up to a UV dose of 630 kWh/m^2.

of photodegradation (see Supporting information, Section 2). Fig. 9 shows the FTIR-ATR spectra of the EVA-100 sample, which clearly underwent a strong degradation. Changes in the absorption peaks were visible starting from UV doses of about 126 kWh/m^2. Notably, a reduction of the peaks at 1020 and 1238 cm^{-1} assigned to the C–O–C stretching vibration of the VA moieties was observed [21]. Concurrently, the rise of the peak at 1160 cm^{-1} indicated severe damage to the concentration of branches of $OCOCH_3$ acetate. This band is characteristic of the vibrational mode of C–O–C groups, which appear from the EVA chain scission [29]. The degradation of VA groups was additionally denoted by the decrease of the C═O peak at 1736 cm^{-1}. This was replaced by the new bands at 1715 and 1720 cm^{-1} assigned to the presence of C═O groups related to ketones generated from Norrish III photolysis reaction [10], and the shoulder at 1780 cm^{-1} of gamma-lactones due to back-biting process. In parallel to the degradation of VA side groups, the ethylene main chain was affected during the UV aging. This was the result of intensity reduction of peaks at 1370, 2850, and 2920 cm^{-1}, assigned to stretching and deformation vibration bands of ethylene and methylene groups. Note that we were able to record FTIR spectra of EVA-100 only up to a total UV dose of 441 kWh/m^2. After this dose, the encapsulant was too brittle to be measured by ATR. These chemical and structural changes closely match with recent works on the degradation of EVA aged by combined UV and high RH stresses [30].

DSC measurements of the EVAs were performed about halfway through the test, after a UV dose of 278 kWh/m^2. Results for the three different EVAs are reported in Fig. 10. Physical aging effects on the polymeric films were visible during the first heating scans: EVA-30 and EVA-65 showed similarities for both secondary and primary crystallization domains. The corresponding melting peaks were set at 46 and 60 °C, respectively, with a CIR of 1.5 (EVA-65) and 1.4 (EVA-30). The appearance of a third melting peak at 86 °C was attributed to the formation of smaller and more perfect ethylene crystals. The EVA samples exposed to temperatures close to the melting region (e.g. 60 °C), could melt and recrystallize [31–33]. EVA-100 did not show any secondary or primary endothermic peaks in the typical 45–65 °C interval. The cooling curves indicate that crystallization peaks are all shifted to higher values with respect to unaged conditions (see Fig. 4), from the initial 40 °C–48 °C for EVA-30, 45 °C for EVA-65, and a smaller exothermic peak at 70 °C for EVA-100. This was attributed to chain scission due to the UV load combined with high humidity levels [33]. In the second

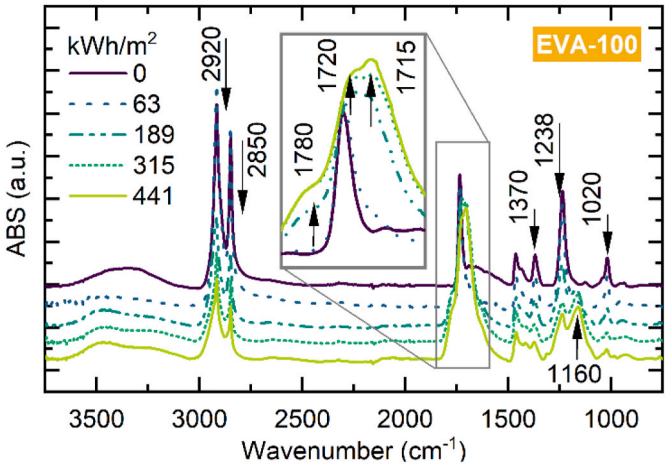

Fig. 9. FTIR-ATR absorption spectra performed on G/ETFE/EVA/G EVA-100 coupons during UV exposure (up to a UV dose of 441 kWh/m^2). Arrows refer to the intensity increase (arrows pointing up) and decrease (arrows pointing down) of the different peaks during UV aging. The zoom in highlights the increase in intensity of the bands at 1715 and 1720 cm^{-1} attributed to ketones formation and at 1780 cm^{-1} assigned to gamma-lactones.

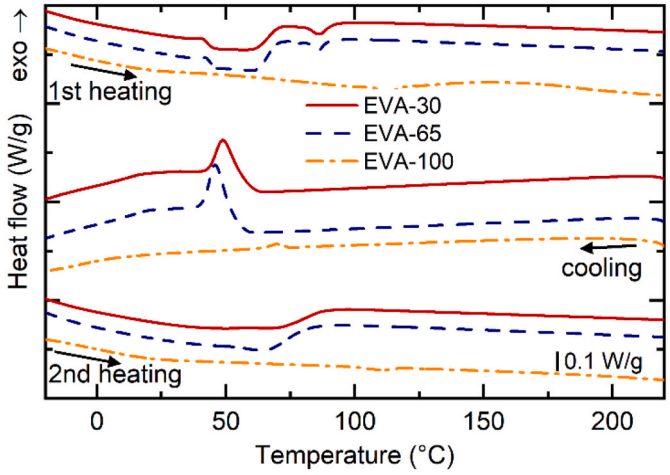

Fig. 10. DSC thermographs performed on the G/ETFE/EVA/G coupons with EVAs stored at different conditions (EVA-30, EVA-65, and EVA-100) during UV aging, after a UV dose of 278 kWh/m^2.

heating thermograph, EVA-30 and EVA-65 exhibited again one single melting peak at 65 and 64 °C, respectively. The comparison with the unaged sample confirmed the better stability of these two samples during UV aging with respect to the EVA-100. No peaks were detectable for EVA-100, indicating a generalized physical and chemical degradation of the polymer and loss of long-range crystal order.

4. Summary and discussion

4.1. Film storage and experimental mid-term UV exposure

Directly after the lamination process, no major notable differences could be observed between the modules encapsulated with optimally or poorly stored EVA. Only some minor physical defects (such as bubble generated along the edges of the modules) were detected by visual inspection. More in-depth material analysis revealed that the moisture from poorly stored EVAs was not entirely outgassed during the lamination process and that residual acidic species were present. DSC measurements demonstrated that both poorly stored EVAs had a comparable crystal morphology, namely, forming a less stable crystal structure after the curing step compared to the optimally stored EVA-30. Nevertheless, this had no direct impact on the IV characteristics of the modules as laminated.

However, we have shown that assumed flawless modules could instead rapidly degrade after installation (i.e. after exposure to UV) because of poor encapsulant storage.

After the exposure of the samples to UV, different aging behaviours were observed. Particularly, the optimally stored EVA (EVA-30) and first poorly stored EVA (EVA-65) reveal no signs of degradation during the whole duration of the experiment. This result was well in accordance with the changes in the crystal morphology observed by DSC: exposure to temperatures close to the melting region of EVA-65 (i.e. the temperature inside the climatic chamber, 65 °C) favoured a rearrangement of the crystal morphology of this sample to resemble the properties of the more stable EVA-30 encapsulant. During the recrystallization process, the residual moisture had been partially outgassed, and this result was attributed to the temperature and not to the UV exposure. Moreover, we emphasize the fact that the performance of the single-cell modules laminated with these polymers (EVA-30 and EVA-65) was very stable up to a cumulative UV dose of 630 kWh/m^2. However, for samples encapsulated with EVA-100, the extreme storage condition in which the roll was soaked in water, the visual inspection of the modules showed that UV exposure resulted in fast degradation of the polymer. New bubbles were generated in the centre of the module, and considerable shrinkage occurred along the edges of the sample. A constant reduction in the current Isc of the modules (and consequently of the power Pmax) was correlated to the increasing yellowing of the encapsulant, starting from a cumulative UV dose of about 189 kWh/m^2. The chemical degradation of the polymer observed by FTIR (Fig. 9) was assigned to the VA moieties chain braking and the generation of ketones and lactones by-products. It also showed severe degradation of the ethylene main chain. Finally, the EVA encapsulant eventually became rigid and brittle due to these multiple chemical and structural changes. Therefore, the results observed for the EVA-100 mini-modules tell us that (i) the water absorbed prior to the lamination process cannot be completely degassed out the module and that (ii) the combination of UV radiation and moisture can already considerably affect module performance on this time scale (the cumulative UV dose reached during the indoor aging test of 630 kWh/m^2 is approximately equivalent to 10 years of outdoor exposure in a mid-latitude country). Therefore, it is sufficient to understand only the early-to mid-life effects of residual trapped water on module degradation.

However, in geographical zones where the humidity levels are not so high during the year (i.e. non tropical climates), these results tend to suggest that EVA can still be a viable solution to encapsulate double-glass PV modules, if good polymer storage and handling practices are carefully respected. On the contrary, if these conditions are not respected, or in the event of module operation in a hot and humid climate (i.e. moisture can gradually diffuse inside the module from the edges) we believe that this may impact the long-term performance of glass-glass c-Si modules encapsulated with EVA. Understandably, in the first case (i.e. if the storage of the encapsulant roll is not optimal), sign of polymer degradation would be evenly spread throughout the module (i.e. modules encapsulated with EVA-100). In the latter case (i.e. module installed in a hot and humid climate) polymer degradation would start from the edges and slowly propagate to the centre, leading to an inhomogeneous degradation pattern.

4.2. Long-term water-ingress modelling

To reach this cumulative UV dose took more than one year of testing. Therefore, to support our previous hypothesis and understand how the modules' potential wear-out mechanism – after 25–30 years of field operation - may look like, we have run some mathematical simulations to model the water ingress inside a 60 6" cells G/G module encapsulated with EVA. Details about water-ingress modelling in PV laminates are contained in previous work [21–23]. We simulated a total exposure of 20 years in two different climates: (1) a hot and humid (i.e in Mumbai, India) and (2) hot and dry one (i.e. in Sharurah, southern Saudi Arabia). The results are reported in Fig. 11. For both climatic regions, the water content as a function of time in three different points in the encapsulant of the laminate was modelled, according to the geometry depicted in Fig. 11a: (i) at the module edge; (ii) at the centre of the first cell (C1), i.e. at a distance of 20 cm from the external edge of the module; and (iii) in the centre of the second cell (C2), i.e. at a distance of 36 cm from the edge. By comparing Fig. 11b and c, we observe that in the case of an installation in a tropical climate, the edge of the module displays a "sinusoidal" trend reflecting the seasonality of the ambient relative humidity. However, the water concentration under the first cell (i.e. point C1 line in Fig. 11b) is not negligible, and moisture can also reach the second cell at a later stage (point C2 line in Fig. 11c). Lower moisture contents for the same structure are modelled in a hot and dry climate, as shown in Fig. 11c. The water concentration at the edges is always more than 50% lower when compared to the tropical climate. Additionally, the seasonality trend for the edge point of the laminate in a hot and dry climate becomes much less significant.

Based on these results, we can consider the adoption of EVA polymers in the manufacturing of glass-glass modules. However, the storage and handling conditions prescribed by the supplier should be carefully respected. These precautions are needed to ensure the use of a high-

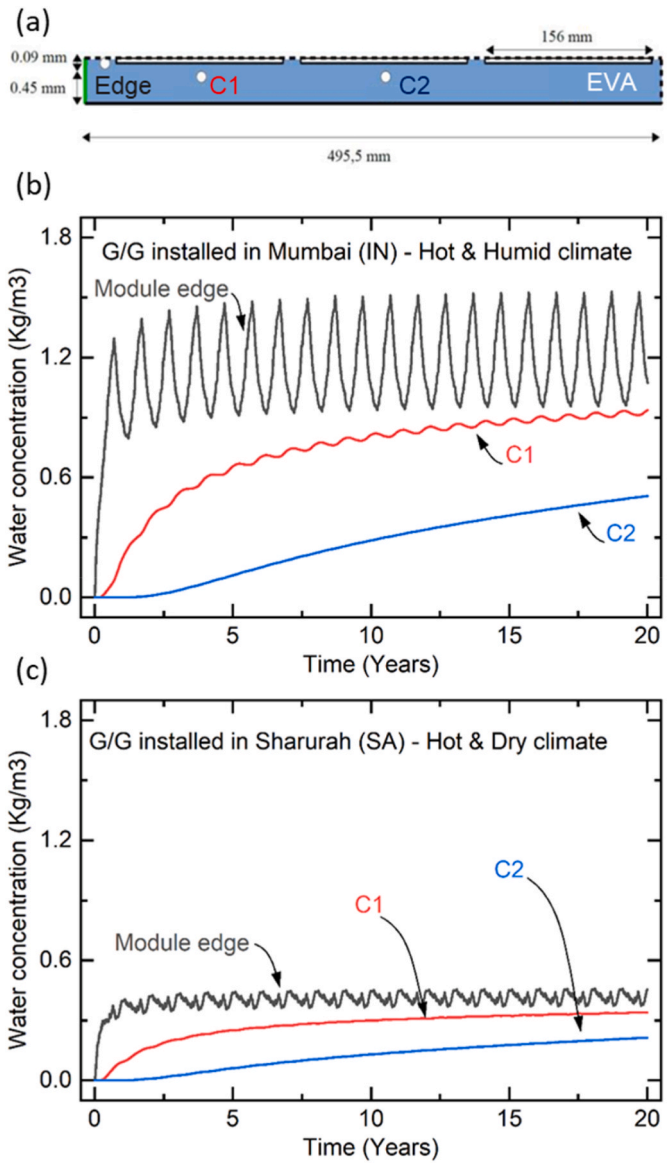

Fig. 11. Modelling the water concentration in a 60-cells G-G module encapsulated with EVA. (a) module schematics with the 3 points at which the water concentration was modelled: module edge, in the middle of the first cell (C1), and in the middle of the second cell (C2). The dashed lines indicate the boundaries where symmetry conditions were assumed. The simulations model the temporal evolution of the water concentration for the exposure in: (b) a hot and humid climate (Mumbai), and (c) a hot and dry climate (Sharurah).

quality material during the fabrication and finally, to deliver a long-term reliable product.

5. Conclusions

This work investigated the potential and criticalities of using EVA as an encapsulant material to manufacture glass-glass solar PV modules. The generation of acetic acid as a by-product of EVA photodegradation combined with a non-fully permeable glass-glass architecture may create a barrier to the adoption of this polymer for glass-glass modules. In the case of an encapsulant material with a high WVTR, as EVA, in fact water may still ingress - with a low kinetics - from the edges. In particular, we simulated the effect of pre-absorbed water by the uncured EVA roll due to an uncontrolled storage environment or daily/seasonal variations in relative humidity that may be experienced in non-optimally controlled manufacturing environment. Then we simulated a UV outdoor exposure of approximately 10 years, which is sufficient to understand the early-to mid-life effects of residual trapped water on module degradation.

Based on our observations, we leave a door open to the adoption of high-quality EVA polymers in the manufacturing of glass-glass modules. However, the storage and handling conditions prescribed by the supplier should be carefully respected. In addition, good manufacturing practices should include:

- When uncured polymer rolls cannot be stored in a controlled environment, it is recommendable to cut only the needed quantity of material and to restore the remaining roll back in the original wrapping – under controlled environmental conditions - to reduce the exposure of the polymer surface to the air.
- When this condition cannot be satisfied, another possibility is to make some modifications to the lamination process steps. One possibility would be to increase the initial pre-heating degas step time to allow potentially trapped water to degas out the module. Alternatively, after the curing step, the cooling step can be extended by leaving modules at a temperature of about 65 °C for longer time so the encapsulant can rearrange the crystal morphology to a more stable form. These adjustments prolong the lamination time, however can significantly improve the long-term stability of the encapsulant, hence the reliability of the module.

CRediT authorship contribution statement

Luca Gnocchi: Writing – review & editing, Writing – original draft, Methodology, Investigation, Formal analysis, Data curation, Conceptualization. **Alessandro Virtuani:** Writing – review & editing, Validation, Supervision, Methodology, Funding acquisition, Conceptualization. **Andrew Fairbrother:** Writing – review & editing, Supervision, Conceptualization. **Eleonora Annigoni:** Writing – review & editing, Investigation, Data curation. **Christophe Ballif:** Writing – review & editing, Validation, Supervision, Project administration, Funding acquisition.

Declaration of competing interest

The authors declare the following financial interests/personal relationships which may be considered as potential competing interests: There are no conflicts to declare: Luca Gnocchi reports financial support was provided by Federal Polytechnic School of Lausanne. Luca Gnocchi reports a relationship with Federal Polytechnic School of Lausanne that includes: employment.

Data availability

Data will be made available on request.

Acknowledgements

The authors gratefully acknowledge Micha Burger and Xavier Niquille for thier help with the experimental work. This work was supported by the H2020 GOPV project that has received funding from the European Union's Horizon 2020 research and innovation programme under grant agreement No 792059.

Appendix A. Supplementary data

Supplementary data to this article can be found online at https://doi.org/10.1016/j.solmat.2023.112526.

References

[1] G. Oreski, B. Ottersböck, A. Omazic, Degradation processes and mechanisms of encapsulants, in: Durability and Reliability of Polymers and Other Materials in Photovoltaic Modules, Elsevier, 2019, pp. 135–152.

[2] R.F. Lange, Y. Luo, R. Polo, J. Zahnd, The lamination of (multi) crystalline and thin film based photovoltaic modules, Prog. Photovoltaics Res. Appl. 19 (2) (2011) 127–133.

[3] R. Kopecek, J. Libal, Bifacial photovoltaics 2021: status, opportunities and challenges, Energies 14 (8) (2021) 2076.

[4] F. Pern, A. Czanderna, Characterization of ethylene vinyl acetate (eva) encapsulant: effects of thermal processing and weathering degradation on its discoloration, Sol. Energy Mater. Sol. Cell. 25 (1–2) (1992) 3–23.

[5] A. Czanderna, F. Pern, Encapsulation of pv modules using ethylene vinyl acetate copolymer as a pottant: a critical review, Sol. Energy Mater. Sol. Cells 43 (2) (1996) 101–181.

[6] F. Pern, Factors that affect the eva encapsulant discoloration rate upon accelerated exposure, Sol. Energy Mater. Sol. Cells 41 (1996) 587–615.

[7] M.C.C. de Oliveira, A.S.A.D. Cardoso, M.M. Viana, V.d.F.C. Lins, The causes and effects of degradation of encapsulant ethylene vinyl acetate copolymer (eva) in crystalline silicon photovoltaic modules: a review, Renew. Sustain. Energy Rev. 81 (2018) 2299–2317.

[8] M.D. Kempe, G.J. Jorgensen, K.M. Terwilliger, T.J. McMahon, C.E. Kennedy, T. T. Borek, Acetic acid production and glass transition concerns with ethylene-vinyl acetate used in photovoltaic devices, Sol. Energy Mater. Sol. Cells 91 (4) (2007) 315–329.

[9] B. Ketola, A. Norris, Degradation Mechanism Investigation of Extended Damp Heat Aged Pv Modules, 26th EUPVSEC, 2011.

[10] J. Jin, S. Chen, J. Zhang, Uv aging behaviour of ethylene-vinyl acetate copolymers (EVA) with different vinyl acetate contents, Polym. Degrad. Stabil. 95 (5) (2010) 725–732.

[11] P. Berlin, Industry Trends in Pv Module Quality from over 250 Factory Audits, 2019.

[12] C. Osterwald, T. McMahon, History of accelerated and qualifcation testing of terrestrial photovoltaic modules: a literature review, Prog. Photovoltaics Res. Appl. 17 (1) (2009) 11–33.

[13] S. Krauter, R. Pénidon, B.R. Lippke, M. Hanusch, P. Grunow, Pv Module Lamination Durability, 2011.

[14] S. Photocap®, Storage conditions for photocap® pv encapsulants [Online], http://www.yumpu.com/en/document/read/13285014/download-str-photocap-r-encapsulant-storage-conditions. (Accessed 10 October 2021).

[15] F.J. Pern, Pv module encapsulation–materials, process, and reliability, in: 16 Th Workshop on Crystalline Silicon Solar Cells and Modules: Materials and Processes, 2006, p. 111.

[16] T.S.E. Malguth, B. Buhl, Fast and non-destructive determination of the eva cross-linking degree for in-line and off-line application, in: 28th European Photovoltaic Solar Energy Conference and Exhibition, 2013, pp. 472–475.

[17] K. Brecl, C. Barretta, G. Oreski, B. Malǐc, M. Topǐc, The influence of the eva film aging on the degradation behavior of pv modules under high voltage bias in wet conditions followed by electroluminescence, IEEE J. Photovoltaics 9 (1) (2018) 259–265.

[18] H. Gong, G. Wang, L. Zheng, M. Gao, Reliability and durability impact of high UV transmission EVA for PV modules, in: 31st European Photovoltaic Solar Energy Conference and Exhibition, EUPVSEC), 2015, pp. 2061–2065.

[19] R. Witteck, H. Schulte-Huxel, B. Veith-Wolf, M.R. Vogt, F. Kiefer, M. Kontges, R. Peibst, R. Brendel, Reducing uv induced degradation losses of solar modules with c-si solar cells featuring dielectric passivation layers, in: 2017 IEEE 44th Photovoltaic Specialist Conference (PVSC), IEEE, 2017, pp. 1366–1370.

[20] A. Sinha, K. Hurst, S. Ulĭcná, L.T. Schelhas, D.C. Miller, P. Hacke, Assessing uvinduced degradation in bifacial modules of different cell technologies, in: 2021 IEEE 48th Photovoltaic Specialists Conference (PVSC), IEEE, 2021, pp. 767–770.

[21] M.D. Kempe, Modeling of rates of moisture ingress into photovoltaic modules, Sol. Energy Mater. Sol. Cell. 90 (16) (2006) 2720–2738.

[22] A. Virtuani, E. Annigoni, C. Ballif, One-type-fits-all-systems: strategies for preventing potential-induced degradation in crystalline silicon solar photovoltaic modules, Prog. Photovoltaics Res. Appl. 27 (1) (2019) 13–21.

[23] M. Jankovec, F. Galliano, E. Annigoni, H.Y. Li, F. Sculati-Meillaud, L.E. Perret-Aebi, M. Topič, In-situ monitoring of moisture ingress in PV modules using digital humidity sensors, IEEE J. Photovoltaics 6 (5) (2016) 1152–1159.

[24] N.S. Allen, M. Edge, M. Rodriguez, C.M. Liauw, E. Fontan, Aspects of the thermal oxidation of ethylene vinyl acetate copolymer, Polym. Degrad. Stabil. 68 (3) (2000) 363–371.

[25] X. Yi, Z. Xu, Y. Liu, X. Guo, M. Ou, X. Xu, Highly efficient removal of uranium (vi) from wastewater by polyacrylic acid hydrogels, RSC Adv. 7 (11) (2017) 6278–6287.

[26] B.K. Sharma, U. Desai, A. Singh, A. Singh, Effect of vinyl acetate content on the photovoltaic-encapsulation performance of ethylene vinyl acetate under accelerated ultra-violet aging, J. Appl. Polym. Sci. 137 (2) (2020), 48268.

[27] B. Ottersböck, G. Oreski, G. Pinter, Comparison of different microclimate effects on the aging behavior of encapsulation materials used in photovoltaic modules, Polym. Degrad. Stabil. 138 (2017) 182–191.

[28] G. Oreski, G.M. Wallner, Damp heat induced physical aging of pv encapsulation materials, in: 2010 12th IEEE Intersociety Conference on Thermal and Thermomechanical Phenomena in Electronic Systems, IEEE, 2010, pp. 1–6.

[29] A. Badiee, R. Wildman, I. Ashcroft, Effect of UV aging on degradation of ethylenevinyl acetate (EVA) as encapsulant in photovoltaic (pv) modules, in: Reliability of Photovoltaic Cells, Modules, Components, and Systems VII, vol. 9179, International Society for Optics and Photonics, 2014, p. 91790O.

[30] C. Barretta, G. Oreski, N. Kyranaki, D.E. Mansour, T.R. Betts, L.P. Bauermann, K. Resch-Fauster, Effects of artificial ageing tests on eva degradation: influence of microclimate and methodology approach, in: 2021 IEEE 48th Photovoltaic Specialists Conference (PVSC), IEEE, 2021, pp. 312–315.

[31] G.W. Ehrenstein, G. Riedel, P. Trawiel, Thermal Analysis of Plastics: Theory and Practice, Carl Hanser Verlag GmbH Co KG, 2012.

[32] J.C. Schlothauer, K. Grabmayer, I. Hintersteiner, G.M. Wallner, B. Röder, Nondestructive 2d-luminescence detection of EVA in aged pv modules: correlation to calorimetric properties, additive distribution and a clue to aging parameters, Sol. Energy Mater. Sol. Cell. 159 (2017) 307–317.

[33] C. Barretta, G. Oreski, S. Feldbacher, K. Resch-Fauster, R. Pantani, Comparison of degradation behavior of newly developed encapsulation materials for photovoltaic applications under different artificial ageing tests, Polymers 13 (2) (2021) 271.